Novel bionanocomposites of poly(vinyl alcohol) and modified chiral layered double hydroxides: Synthesis, properties and a morphological study

Shadpour Mallakpour [a,b,*], Mohammad Dinari [a,b]

[a] Organic Polymer Chemistry Research Laboratory, Department of Chemistry, Isfahan University of Technology, Isfahan 84156-83111, Islamic Republic of Iran
[b] Nanotechnology and Advanced Materials Institute, Isfahan University of Technology, Isfahan 84156-83111, Islamic Republic of Iran

ABSTRACT

The effect of novel modified layered double hydroxides (LDHs) on thermal and structural properties of poly(vinyl alcohol) (PVA) was investigated. Organically modified chiral LDH was prepared via ion exchange reaction of LDH in a solution of *N,N′*-(pyromellitoyl)-bis-L-phenylalanine diacid in distilled water. The modified Mg-Al LDH materials showed an increase in interlayer distance as compared to the unmodified Mg-Al LDH by X-ray diffraction (XRD). Bionanocomposites of PVA with the modified chiral LDH were prepared with different compositions of LDH by solution-intercalation method using the ultrasound-assisted technique. The effect of LDH contents on thermal, physicomechanical, and morphological properties of PVA films was investigated using XRD, Fourier transform infrared, thermogravimetric analysis (TGA), field emission scanning electron microscopy and transmission electron microscopy techniques. The TGA of the obtained bionanocomposites showed an increase in thermal stability. The uniform distribution of clay due to the intimate interaction between clay and polymer appeared to be the reason for the improved properties.

© 2013 Elsevier B.V. All rights reserved.

1. Introduction

Layered double hydroxides (LDHs), which are widely known as host–guest materials, are a significant class of naturally occurring minerals whose synthesis in the lab is easily accessible [1,2]. Such materials, also known as anionic clays, have the capability of anion swelling, making them very versatile. In addition to the rich intercalation chemistry that can be played with, it also shows a wide range of variations in its composition. This latter aspect is based on the versatility of the general formula $[M^{2+}_{1-x} M^{3+}_x (OH)_2](A^{m-})_{x/m} \cdot nH_2O$, where both M^{2+} and M^{3+} can be varied, and A^{m-} is usually a simple anion such as Cl^-, NO_3^- or CO_3^{2-}. In its general formula, x measures the amount of M^{3+} relative to $(M^{3+} + M^{2+})$, correlating with the spacing between layers. Their structure is based on brucite-like layers, where a divalent metal cation is located in the center of oxygen octahedral and two-dimensional infinite layers are formed by edge-sharing of octahedral. Moreover, the spacing is changed concomitantly by both the size of the intercalated anions and the degree of hydration [1,3–7].

The lamellar structure and anion exchange properties of LDHs make them attractive for technological applications such as ion-exchangers, adsorbent materials, pharmaceutical stabilizers, and precursors for new catalytic materials [8–11]. LDH, due to its layered structure, is an attractive choice as nanofiller considered for the preparation of multifunctional polymer/layered crystal nanocomposites (NCs). However, its use as a nanofiller is limited by its high-charge density, and the high content of anionic species and water molecules, all resulting in strong interlayer electrostatic interactions between the sheets and pronounced hydrophilic properties. Consequently, it is difficult for a monomer or polymer to penetrate into the LDH layers or the LDH layers to be homogeneously dispersed within hydrophobic polymer matrices. To facilitate the intercalation of polymer in the layers of LDH, or to achieve a good degree of the layer dispersion in polymer matrices, the interlayer space should be modified with suitable organic anions for the purpose of increasing both the interlayer distance and the hydrophobicity of LDH layers [12–16].

Anions are typically intercalated into LDH interlayers by three approaches [1,17]. The first approach is the coprecipitation method, which requires the addition of a solution of M^{2+} and M^{3+} ions into a base solution of the desired anions. The second technique is the

* Corresponding author at: Organic Polymer Chemistry Research Laboratory, Department of Chemistry, Isfahan University of Technology, Isfahan 84156-83111, Islamic Republic of Iran. Tel.: +98 311 391 3267; fax: +98 311 391 2350.

E-mail addresses: mallak@cc.iut.ac.ir,
mallak777@yahoo.com, mallakpour84@alumni.ufl.edu (S. Mallakpour).

direct ion exchange method, in which LDHs are stirred in a solution of the chosen anions at a suitable concentration. The last method is the rehydration method in which the calcined LDH is added to a solution of desired anions [18]. The selection of anions for the modification of LDH depends on the next application of LDH. For example, Mg–Al LDHs intercalated with dodecylsulfate and dodecylbenzenesulfonate have been used to adsorb pesticides, such as triadimefon, linuron, atrazine, acephate, and diazinon from aqueous solution [19,20]. Also, LDHs containing interlayer carboxylate anions have attracted considerable attention in recent years due to interesting properties and potential applications, e.g., LDH modified with citrate, malate, and tartrate ions are able to take up hazardous organic materials and heavy metal ions from an aqueous solution [21].

Polyvinyl alcohol (PVA), a polyhydroxy polymer, is a thermoplastic and biocompatible petroleum based polymer. It is also one of the rare polymers with a carbon–carbon single bond backbone that is fully biodegradable [22,23]. Because of the hydroxyl (—OH) groups on alternating carbon atoms, PVA is strongly hydrophilic and soluble in water, helping to promote its degradation through hydrolysis [24]. PVA has been largely studied owing to its good film forming ability, high hydrophilicity, biocompatibility, good chemical resistance and interesting mechanical properties. These properties have led to a wide range of industrial products such as membrane, textile sizing and finishing, adhesive, coatings, paints and as a protective colloid for emulsion polymers [25–28]. Lately, the interest has been focused on its promising biomedical applications such as drug delivery systems, dialysis membrane; wound dressing, scaffolds for tissue engineering, contact lenses, and artificial organs [27,28]. These applications have encouraged researchers to improve thermal, mechanical and barrier properties of NC films, while retaining the optical clarity of PVA. This polymer is the most commercially important water soluble plastic which has been extensively investigated as a matrix for different kinds of nanofillers [26–29]. PVA is sold by the major chemical companies as a clear granular material in a variety of molecular weights. These properties have led to its broad industrial use [30].

More recently, PVA and LDH based NCs have been developed to improve PVA's properties and further explore its applications by solution casting process [31–36]. LDH based NCs have shown the exfoliated nature of the dispersed particles. Inspired by these studies, this work has focused on investigating the properties of PVA and chiral modified LDH (MLDH) bionanocomposites (BNCs) by solution casting method for the first time. The chiral dicarboxylate anion of N,N′-(pyromellitoyl)-bis-phenylalanine diacid was prepared in NaOH solution. Different amounts of this novel MLDH were used for the synthesis of PVA/MLDH BNCs. The properties of the hybrids were studied in the film form as a function of the MLDH contents in the polymer matrix. This also examined the relationship between the properties and structures of the organoclay and PVA/nanoclay hybrid films with X-ray diffraction (XRD), Fourier transfer infrared (FTIR) and thermogravimetric analysis (TGA) techniques. The morphology of obtained materials was examined by field emission scanning electron microscopy (FE-SEM) and transmission electron microscopy (TEM).

2. Experimental

2.1. Materials

PVA (99% hydrolysis, weight-average molecular weight = 72,000 g/mol), L-phenylalanine amino acid ($C_6H_{13}NO_2$, 131.18 g/mol, ≥99%), Pyromellitic dianhydride and sodium hydroxide (NaOH) were purchased from Merck Chemical Co. Hydrotalcite; ($Mg_6Al_2(CO_3)(OH)_{16}\cdot4(H_2O)$) was purchased from Sigma–Aldrich Co.

2.2. Characterization techniques

The reaction was carried out on a MISONIX ultrasonic liquid processors, XL-2000 SERIES. Ultrasound was a wave of frequency 2.25×10^4 Hz and power of 100 W.

FT-IR spectra were recorded on Jasco-680 (Japan) spectrophotometer with 2 cm^{-1} resolution. The KBr pellet technique was applied to monitor changes in the FT-IR spectra of the samples in the range of 4000–400 cm^{-1}. The vibrational transition frequencies have been reported in wavenumbers (cm^{-1}).

The interlayer spacing of the organoclays was measured by an XRD (Bruker, D8 Advance, Germany) with Cu $K\alpha$ radiation (λ = 0.1542 nm) at 45 kV and 100 mA. The diffraction patterns were collected between 2θ of 1.2° and 80° at a scanning rate of 0.05/min. Basal spacing was determined from the position of the $d(0\,0\,1)$ reflection. The scanning speed was 0.02/s. The d-spacing of the organic montmorillonite was analyzed using Bragg's equation ($n\lambda = 2d \sin\theta$). Where n is an integer, λ is the wavelength, θ is the glancing angle of incidence, and d is the interplanar spacing of the crystal.

TGA was performed on an STA503 WinTA instrument in a nitrogen atmosphere by the heating rate of 10 °C/min from ambient temperature to 800 °C at the nitrogen atmosphere.

The morphology of the MLDH and BNCs was examined by FE-SEM (HITACHI; S-4160). The powdered sample was dispersed in H_2O, and then the sediment was dried at room temperature before gold coating.

The dispersion of the nanoclay within the medium was controlled by TEM. The TEM images were obtained from a Philips CM120 using an accelerator voltage of 100 kV. The inorganic components appeared black/gray on the micrographs.

2.3. Synthesis of chiral LDH

The preparation was performed in a nitrogen atmosphere to exclude carbon dioxide, whose presence could lead to the formation of a carbonate LDH. N,N′-(pyromellitoyl)-bis-L-phenylalanine diacid pillared LDH was prepared by adding superfluous diacid (2.5 g) to a suspension of the LDH in 100 ml of distilled water. The suspension was slowly dissolved with effervescence and a clear solution was obtained. This solution was added dropwise to an alkaline solution (NaOH, 2.0 g) in 100 ml of distilled water and the pH was maintained above 9. The resulting white precipitate was aged for 24 h at 65 °C, and then filtered until all of the supernatant liquid was removed. The sample was washed several times with large amounts of distilled water, and then dried at 70 °C in a vacuum oven to give the modified chiral LDH.

2.4. Synthesis of PVA/MLDH BNCs

PVA/MLDH BNCs were synthesized by a solution-intercalation method using ultrasound energy: At first, distilled water was mixed with MLDH to form clay/water suspension of ≤2.5% concentration. The suspension was stirred for 3 h at 40 °C and sonicated for 1 h. Then, low-viscosity, fully hydrolyzed PVA was added to the stirred suspensions to make the total solid (silicate plus polymer) concentration w = 5%. The mixture was then heated to 90 °C for 6 h to dissolve PVA. The mixed solution was condensed and the total solid concentration was controlled at w = 10%. After being sonicated for 1 h, the final films were made via casting on a Petri dish in a closed oven at 40 °C for 24 h; the thickness of the films was controlled from 0.15 to 0.3 mm.
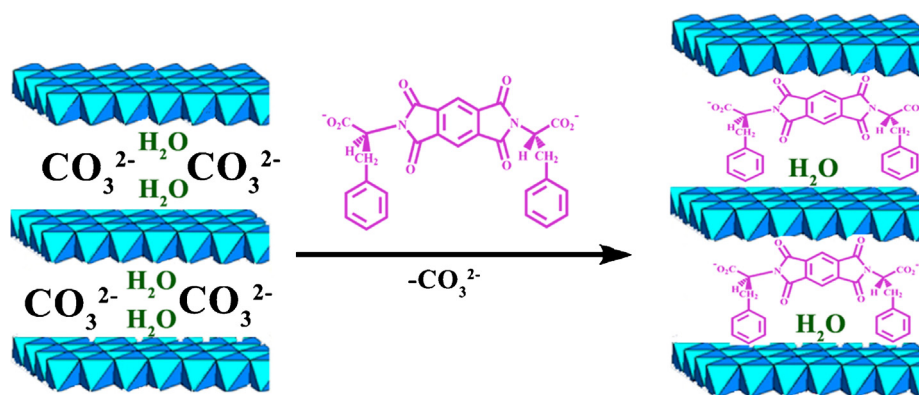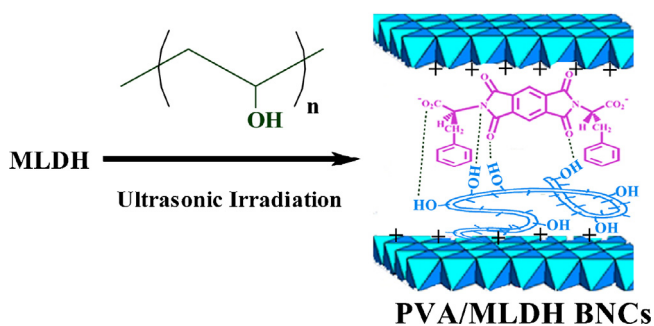
Fig. 1. Preparation of chiral MLDH.

Fig. 2. Possible interaction between PVA and MLDH.

Fig. 3. FT-IR spectra of the samples.

3. Results and discussion

3.1. Preparation of the modified chiral LDH and PVA/modified LDH BNCs

Amino acids are the components of enzymes and proteins. If amino acids or amino acid based materials can be immobilized in the interlayer region, new types of catalytic active compounds with selective reactivity and biomolecule carrier materials can be created. In this study, N,N′-(pyromellitoyl)-bis-L-phenylalanine diacid with the specific rotation $[\alpha]_D^{25} = +0.2$ (measured at a concentration of 0.5 g/dL in DMF at 25 °C) was synthesized according to our previous study [37]. Then, this compound was used for the preparation of the new chiral MLDH. On the other hand, if amino acids are chiral, then the nanohybrids are not only well-defined structures with huge pore openings, but also they create a chiral environment. The spatial orientations of the chiral dicarboxylate/LDH are shown in Fig. 1. As a possible model, chiral dicarboxylate was considered to be arranged vertically or horizontally to the LDH basal layer as shown in Fig. 1. This figure only serves to emphasize the process of adsorption and does not provide information on the order in which the adsorbent molecules were present along with carboxylate ions ionically bound on the surface.

Since PVA has a strong tendency to form hydrogen bonding within itself as well as with other species containing highly electronegative groups, this biodegradable compound was used for the synthesis of the new hybrid materials. The adsorption of PVA onto the surfaces of MLDH was presumed to occur through hydrogen bonding. Apart from hydrogen bonding, van der Waals forces between polymer segments and MLDH surface would also play an important role in the overall adsorption process (Fig. 2).
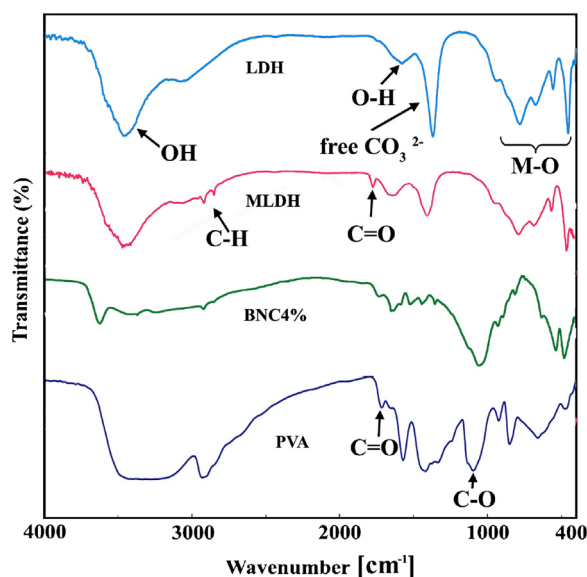
3.2. Characterization

3.2.1. FT-IR study

LDH containing CO_3^{2-} anions had characteristic bands for various modes of infrared sensitive vibrations of the anion. The broad band in the range 3200–3700 cm^{-1} was due to the O—H stretching vibration of the metal hydroxide layer and interlayer water molecules. A shoulder present around 3000–3100 cm^{-1} was caused by the interaction between the CO_3^{2-} and H_2O present in the interlayer region, which involved mostly hydrogen bonds [38]. The bending vibration of the interlayer H_2O was also reflected in the broad bands around 1590 cm^{-1}. The band characteristic to metal-oxygen bond stretching appeared below 700 cm^{-1}. The sharp bands around 780, 554 and 440–450 cm^{-1} were caused by various lattice vibrations associated with metal hydroxide sheets (Fig. 3).

The FT-IR spectrum of MLDH showed two types of bands: one corresponded to the anionic species intercalated and the other to the host LDH materials (Fig. 3). The band around 447 cm^{-1} resulted from the lattice vibration of the hydroxide sheet and the broad band in the range 3200–3700 cm^{-1} was mainly due to O—H groups of the hydroxide layers. The appearance of characteristic bands for CO_3^{2-} indicated that still some CO_3^{2-} existed in the interlayer region. In addition to carbonate ions retained during the calcination process, carbonate ions could be adsorbed during the regeneration process from the atmospheric CO_2 dissolved in the dispersion medium.
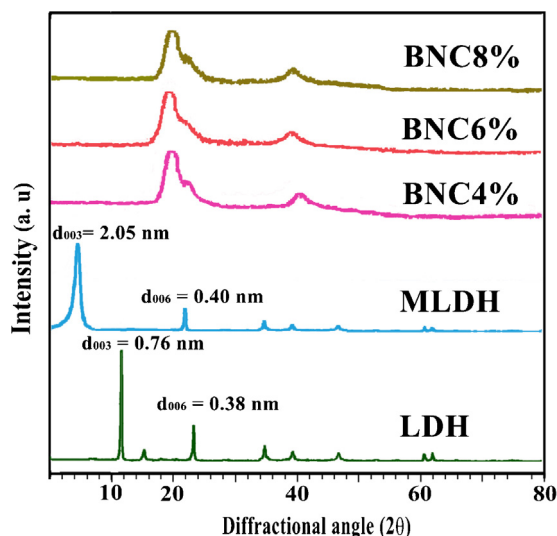
Fig. 4. XRD patterns of different samples.

However, a broad band or shoulder was observed in all modified samples in the range 1600–1640 cm^{-1}, probably indicating the presence of H_2O molecules as bending vibration appeared in this region. The absorption bands at 2930–3100 cm^{-1} corresponded to the ν_{asym} and ν_{sym} (C—H) modes of CH_2 group in the chiral dicarboxylate molecules. The other dicarboxylate bands originated from various functional groups also found at 1740–1700 cm^{-1} (C=O), 1300–1000 cm^{-1} (C—O), and 1600–1475 cm^{-1} (conjugate C=C). The band broadening by intercalation resulted from the electrostatic interaction between chiral diacid molecules and hydroxide sheets, suggesting their safe stabilization in the interlayer space of LDH.

Pure PVA showed a broad absorption peak around 3100–3500 cm^{-1}, which was due to the presence of hydroxyl group of PVA molecules and the adsorbed water. The absorption peaks in the region of 2942 cm^{-1} were due to stretching vibrations of –CH and CH_2 groups and at 1420 cm^{-1} probably corresponded to the vibration of CH_2 bond in PVA molecules (Fig. 3). The band observed at 1713 cm^{-1} was as a result of the carbonyl functional groups of residual acetate groups remaining after the manufacture of PVA from the hydrolysis of poly(vinyl acetate). In BNC4%, the presence of the typical bands of pure PVA and MLDH was confirmed in this spectrum (Fig. 3).

3.2.2. X-ray diffraction

The XRD analysis was used as a very useful method to describe the extent of intercalation and exfoliation of the nanofiller having the layered structure. The complete or high degree of exfoliation of the layered crystalline filler in polymer matrix certainly meant the disappearance of the corresponding peaks from the XRD spectrum. The XRD spectra of pristine LDH, MLDH and PVA/MLDH BNC films containing 2, 4, 6, and 8 wt % of LDH are shown in Fig. 4. The XRD spectrum of Mg-Al LDH showed that this compound had a highly crystalline nature and the layered geometry. The position of the basal peak at $2\theta = 11.84$ indicated that the distance between the two adjacent metal hydroxide sheets was about 0.76 nm. As expected, the position of the basal reflections of the modified sample was shifted to the higher d value, indicating the expansion in the interlayer distance (Fig. 4). The modified sample did not show a distinct reflection at $d = 0.76$ nm. The XRD patterns of the MLDH showed the expanding LDH structure with a sharp (0 0 3) spacing of 2.05 nm in Fig. 4.

The XRD patterns of PVA/MLDH BNCs (4%, 6% and 8%) were characterized by the disappearance of the diffraction peaks corresponding to the LDH irrespective of the variation in the LDH content. The only new broad diffraction peak that appeared at $2\theta = 19.60$ corresponded to the PVA polymer matrix. This complete disappearance of LDH peaks could be due to the partial exfoliated structure, in which the gallery height of intercalated layers was large enough and the layer correlation was not detected by X-ray diffractometer (Fig. 4). Although XRD provides a partial picture on the distribution of the nanofiller and disappearance of the peak corresponding to d-spacing, it does not always confirm the exfoliated NCs, and a complete characterization of NC morphology requires microscopic investigation.

3.2.3. FE-SEM

FE-SEM and TEM observations were used to further confirm the delamination behavior and visualize the morphology of the MLDH nanosheets and PVA/MLDH BNCs. The FE-SEM micrographs of pure LDH, MLDH, and PVA/MLDH BNC containing 8 wt% of MLDH nanoparticles are shown in Fig. 5. The FE-SEM image of pure LDH reveals the nature of LDH particles, which roughly consisted of plate-like shape stacked on the top of each other with lateral dimensions ranging over few micrometers and thickness being over few hundred nanometers. The morphological feature of the MLDH was similar to that of the unmodified LDH. It appeared more floppy compared to the unmodified LDH. The FE-SEM images of PVA/MLDH BNC8% showed that the morphology was changed. This morphological change could be attributed to the re-ordered crystalline phase of the PVA matrix in the presence of the modified LDH, causing a packed network. Apparently, it seems that the particles were distributed uniformly in the polymer matrix.

3.2.4. TEM

TEM was used to directly view the hybrid structure for the NCs formed, with the emphasis on the dispersion of the nanometer-thin layered fillers in the polymer matrix. TEM presented an actual image of nanoclay platelets to permit the identification of the internal morphology of BNCs. Typical TEM images of MLDH and BNC of PVA and 8 wt% of MLDH are shown in Fig. 6. For MLDH, the platelets had a hexagonal shape with rounded corners. There were no signs of aggregation visible in the micrographs. Extensive TEM observations of BNC8% revealed the coexistence of organo-nanosilicate layers in the intercalated and partially exfoliated states. TEM micrograph (Fig. 6d–f) showed two-dimensional objects oriented largely parallel to the grid surface and the thin sheet-like object with similar lateral dimensions. The sheets showed a very homogeneous contrast, reflecting their ultrathin nature and uniform thickness. TEM observations revealed the coexistence of organo-nanosilicate layers in the intercalated and partially exfoliated states.

3.2.5. Thermal degradation characteristics

The comparison of the TGA plots of the MLDH with that of the unmodified one gives an indication of how the interlayer surfactants anions influence the decomposition of the host material. The thermal behavior of the unmodified Mg-Al–LDH has been studied in details by several researchers [39,40]. The most widely reported study suggests a two-stage decomposition process: a low temperature (up to about 225 °C) dehydration stage due to the loss of interlayer water and a high temperature decomposition (225–500 °C) stage due to the loss of interlayer carbonate and dehydroxylation of the metal hydroxide layer. The thermal decomposition analysis of the unmodified LDH and its modified forms is presented in Figs. 7 and 8. The low temperature decomposition step in the unmodified LDH lied below 230 °C with the decomposition peak around 210 °C. During this step, the loss of interlayer water molecules corresponded to a small (about 10–11 wt%) weight loss in the TGA plot. The high temperature decomposition of the unmodified LDH took place in two distinct steps with the decomposition
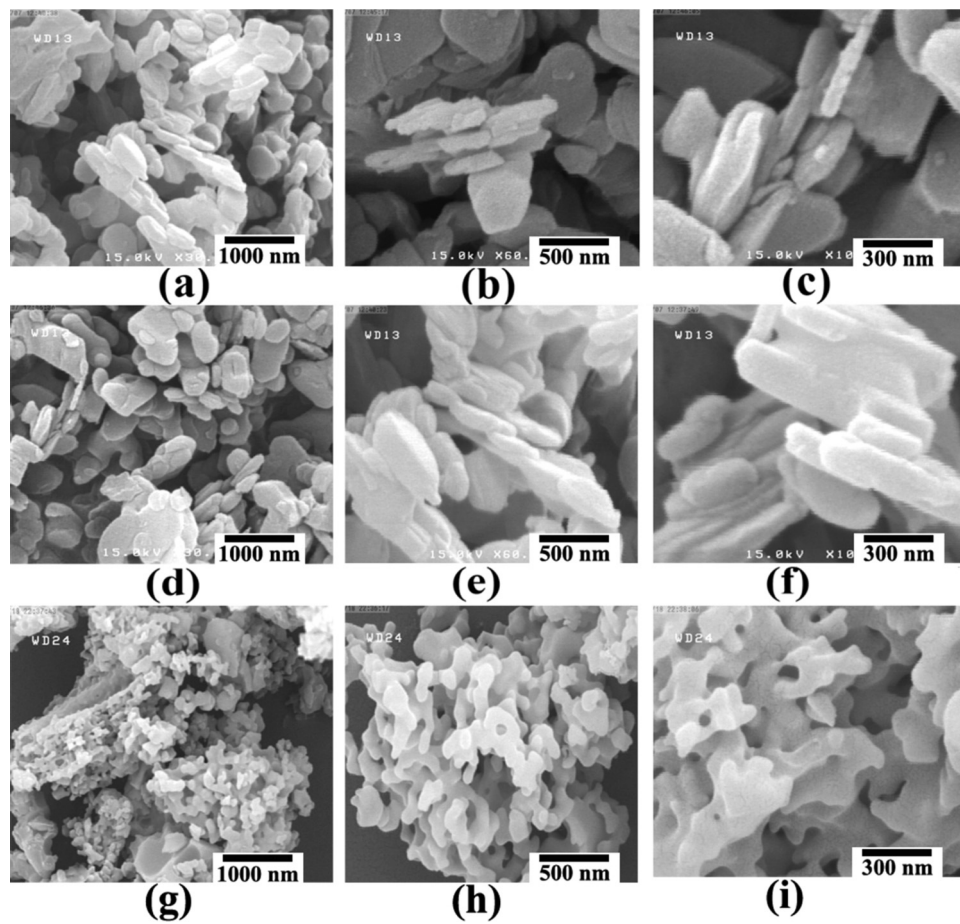
Fig. 5. FE-SEM photographs of LDH (a–c), MLDH (d–f) and PVA hybrid with 8 wt% MLDH (g–i).
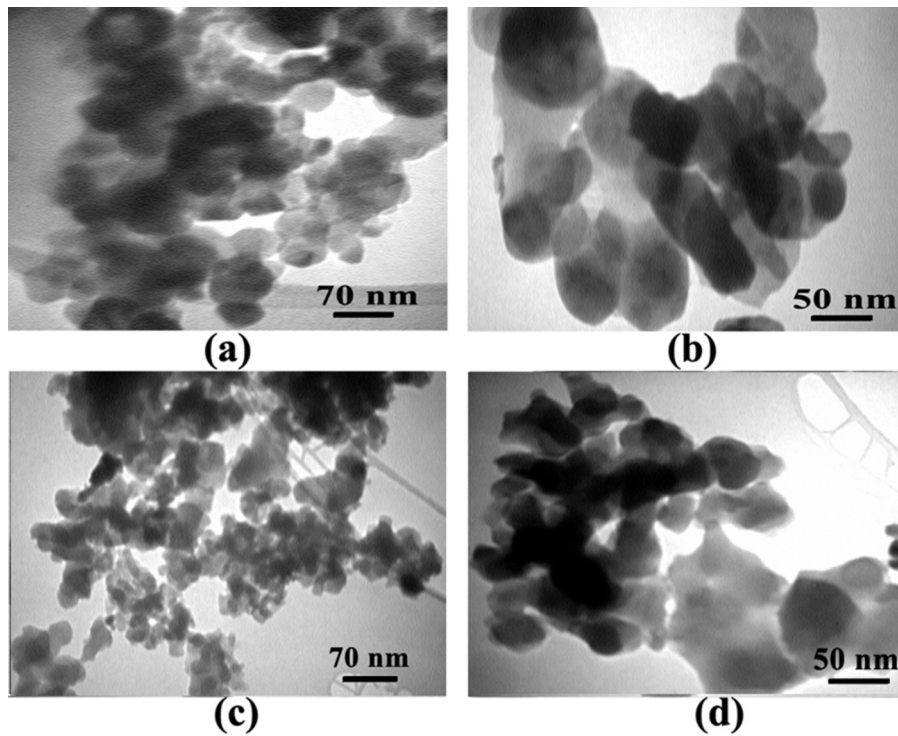

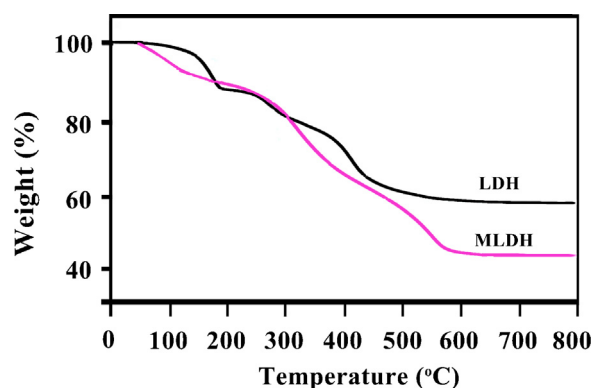**Fig. 6.** TEM micrographs of MLDH (a and b) and PVA hybrids containing 8 wt% of MLDH (c and d).

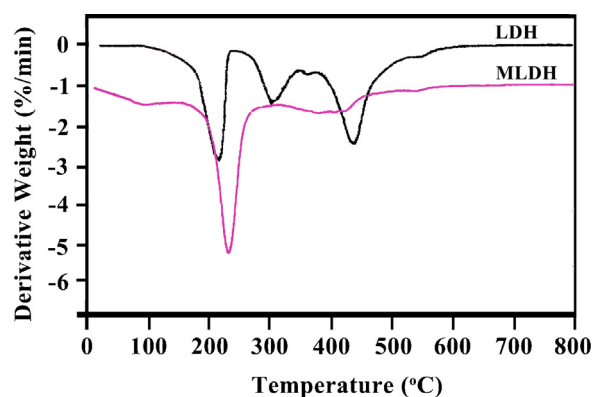**Fig. 7.** TGA thermograms of LDH and MLDH with chiral dicarboxylate.

Fig. 8. DTG thermograms of pristine LDH and MLDH.

Table 1
TGA of neat PVA and different PVA/MLDH BNCs-residual masses at different temperatures.

Temperature (°C)	% Residual mass				
	Neat PVA	BNC2%	BNC4%	BNC6%	BNC8%
200	97.7	98.0	98.0	98.1	98.1
300	58.6	65.8	78.2	81.1	83.2
400	22.6	28.9	34.5	37.2	38.6
500	12.7	17.7	20.3	22.8	23.6
600	8.7	16.4	18.6	19.8	20.1
700	7.1	15.3	18.2	19.6	20.1
800	7.1	15.1	18.2	19.5	20.1

peaks around 300 and 430 °C. The organic modification of the LDH changed its thermal decomposition behavior in comparison to the unmodified sample, especially the second stage of the decomposition process, which resulted in the complete collapse of materials structure [39,40].

The DTG curves of the neat LDH and its modified form with chiral dicarboxyalte are presented in Fig. 8. Thermal degradation of both organically-modified and unmodified LDHs, which is quite well understood, proceeded via three or four steps [41–43]. The first step, below 150 °C, was assigned to the loss of the adsorbed water, followed by the loss of intralayer water between 150 and 250 °C. The last two steps, above 250 °C, were due to dehydroxylation and loss of the gallery anions, respectively. These two steps may overlap (Fig. 8).

The thermal stability of the BNCs of PVA and different amounts of MLDH (2, 4, 6 and 8%) were also investigated by TGA under an N_2 flow. The results are summarized in Table 1 and Fig. 9. The improvement of thermal properties, compared to the unfilled polymer, was a very important aspect of polymer/LDH NCs. LDHs contained a
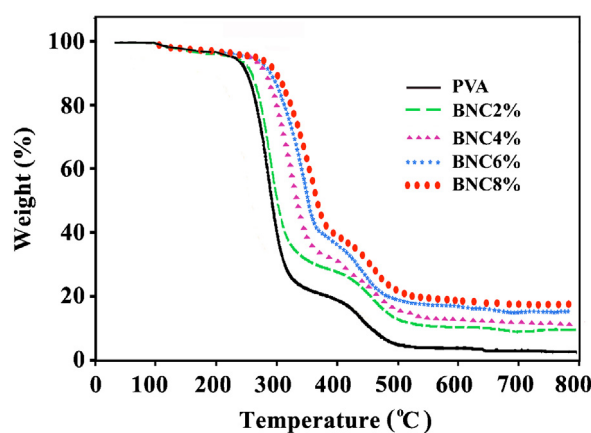

Fig. 9. TGA thermograms of PVA and PVA/MLDH BNCs.

large amount of bound water due to the presence of −OH group on the metal hydroxide sheets and some free water molecules in the interlayer region. The mechanism by which LDH clays improved the thermal stability and flammability of polymer matrix was similar to that observed in the case of conventional metal hydroxide type fillers, like $Mg(OH)_2$ and $Al(OH)_3$ [44,45]. The endothermic decomposition of LDHs took off heat from the surrounding and the liberated water vapor reduced the concentration of the combustible volatile in the vicinity of the polymer surface. As a result, the decomposition temperature of the polymer was increased.

In Fig. 9, the TGA thermograms of PVA, and four samples with 2, 4, 6 and 8 wt% of LDH are compared. In the case of PVA and its composites, three degradation steps can be observed. The first weight loss process, which was associated with the loss of the absorbed moisture, [46] was independent of the concentration of LDH for all samples. All samples presented the same degree of the absorbed water, as inferred from the thermograms, showing that the moisture levels for all the samples were almost similar. The second weight loss process corresponded to the degradation of the PVA by the dehydration reaction of the polymer chain (side chain) [45]. The BNC films showed higher resistance toward thermal degradation. As can be seen from Table 1, PVA film showed 7% residue at 800 °C while the BNC films had 15–20% residue at this temperature. It is notable that even small amounts of clay were effective in improving the weight residues of the hybrids.

4. Conclusions

Organically-modified chiral LDH was prepared via ion exchange reaction of LDH and N,N′-(pyromellitoyl)-bis-L-phenylalanine diacid in distilled water. The modified Mg-Al LDH materials showed an increase in the interlayer distance as compared to the unmodified LDH by XRD. PVA/MLDH BNCs were synthesized with different compositions, 0, 2, 4, 6, and 8 wt% of MLDH, to study the effect of the MLDH concentration on the properties of the PVA/LDH films by a solution-intercalation method using the ultrasound energy. The BNC films were investigated by TGA, XRD and FT-IR. The FTIR analysis showed a good interaction between the continuous PVA matrix and the LDH nanoparticle filler by hydrogen bonding through hydroxyl groups. The morphology of the MLDH and PVA/MLDH BNCs was examined by FE-SEM and TEM and the results indicated that the LDH platelets were well-distributed within the PVA matrix and oriented along the PVA axis in a disorderly fashion. The thermal stability from TGA measurements was shown to be enhanced compared with that of pure PVA. The improvement of thermal properties was attributed to the homogeneous dispersion of MLDHs in polymeric matrix and the strong hydrogen bonding

between O—H groups of PVA and the oxygen atoms of silicate layers or carbonyl group as well as other polar groups of intercalated chiral dicarboxylated anion.

Acknowledgements

References

[1] P.S. Braterman, Z.P. Xu, F. Yarberry, in: S.M. Auerbach, K.A. Carrado, P.K. Dutta (Eds.), Handbook of Layered Materials, Marcel Dekker, Inc., New York, 2004, pp. 373–474 (Chapter 8).
[2] P.D. Vaz, C.D. Nunes, New J. Chem. 34 (2010) 541–546.
[3] U. Costantino, V. Ambrogi, M. Nocchetti, L. Perioli, Microporous Mesoporous Mater. 107 (2008) 149–160.
[4] L. Desigaux, B.M. Belkacem, P. Richard, J. Cellier, P. Leone, L. Cario, C. Taviot-Gueho, B. Pitard, Nano Lett. 6 (2006) 199–204.
[5] M. Wei, J. Guo, Z. Shi, Q. Yuan, M. Pu, G. Rao, X. Duan, J. Mater. Sci. 42 (2007) 2684–2689.
[6] D. Zhao, Z. Bai, F. Zhao, Mater. Res. Bull. 47 (2012) 3670–3675.
[7] M. Meyn, K. Beneke, G. Lagaly, Inorg. Chem. 29 (1990) 5201–5207.
[8] T.Y. Tsai, S.W. Lu, Y.P. Huang, F.S. Li, J. Phys. Chem. Solids 67 (2006) 938–943.
[9] G. Wu, L. Wang, D.G. Evans, X. Duan, Eur. J. Inorg. Chem. 2006 (2006) 3185–3196.
[10] E. Mahboobeh, W. Md, Z.W. Yunus, Z. Hussein, M. Ahmad, N.A. Ibrahim, J. Appl. Polym. Sci. 118 (2010) 1077–1083.
[11] T. Kuila, S.K. Srivastava, A.K. Bhowmick, J. Appl. Polym. Sci. 111 (2009) 635–641.
[12] H.B. Hsueh, C.Y. Chen, Polymer 44 (2003) 1151–1161.
[13] J.E. Moreyon, A. De Roy, C. Forano, J.P. Besse, Appl. Clay Sci. 10 (1995) 163–175.
[14] Z. Matusinovic, M. Rogosic, Polym. Degrad. Stab. 94 (2009) 95–101.
[15] F.P. Jiao, X.Q. Chen, Z.D. Fu, Y.H. Hu, Y.H. Wang, J. Mol. Struct. 92 (2009) 1328–1332.
[16] W.G. Hou, Z.L. Jin, Colloid Polym. Sci. 285 (2007) 1449–1454.
[17] C. Forano, T. Hibino, F. Leroux, C. Taviot-Gueho, in: F. Bergaya, B.K.G. Theng, G. Lagaly (Eds.), Developments in Clay Science, Elsevier, New York, 2006, pp. 1021–1095.
[18] H.W. Olfs, L.O. Torres-Dorante, R. Eckelt, H. Kosslick, Appl. Clay Sci. 43 (2009) 459–464.
[19] M.V. Villa, M.J. Sanchez-Martin, M.J. Sanchez-Camazano, Environ. Sci. Health, Part B: Pestic. Food Contam. Agric. Wastes 34 (1999) 509–516.
[20] T. Tanaka, S. Nishimoto, Y. Kameshima, J. Matsukawa, Y. Fujita, Y. Takaguchi, M. Matsuda, J. Solid State Chem. 183 (2010) 479–484.
[21] T. Kameda, H.Y. Takeuchi, T. Oshioka, J. Phys. Chem. Solids 70 (2009) 1104–1108.
[22] S.R. Kanatt, M.S. Rao, S.P. Chawla, A. Sharma, Food Hydrocolloids 29 (2012) 290–297.
[23] K. Qiu, A.N. Netravali, Compos. Sci. Technol. 72 (2012) 1588–1594.
[24] E.S. Stevens, Green Plastics: An Introduction to the New Science of Biodegradable Plastics, Princeton University Press, Princeton, NJ, 2002, pp. 10–30.
[25] M. Kobayashi, J. Toguchida, M. Oka, Biomaterials 24 (2003) 639–646.
[26] S. Wang, Q. Zhang, B. Tan, L. Liu, L. Shi, J. Macromol. Sci. B: Phys. 50 (2011) 2307–2317.
[27] J.H. Park, H.W. Lee, D.K. Chae, W. Oh, J.D. Yun, Y. Deng, J.H. Yeum, Colloid Polym. Sci. 287 (2009) 943–950.
[28] S. Mallakpour, M. Dinari, J. Appl. Polym. Sci. 124 (2012) 4322–4330.
[29] S. Mallakpour, A. Barati, Polym. Plast. Technol. Eng. 51 (2012) 321–327.
[30] V. Goodship, D. Jacobs, Polyvinyl Alcohol: Materials, Processing and Applications, Smithers Rapra Technology, United Kingdom, 2005.
[31] B. Li, Y. Hu, R. Zhang, Z. Chen, W. Fan, Mater. Res. Bull. 38 (2003) 1567–1572.
[32] B. Ramaraj, S.N. Jaisankar, Polym. Plast. Technol. Eng. 47 (2008) 733–738.
[33] S. Huang, X. Cen, H. Peng, S. Guo, W. Wang, T.J. Liu, Phys. Chem. B 113 (2009) 15225–15230.
[34] C.X. Zhao, Y. Liu, D.Y. Wang, D.L. Wang, Y.Z. Wang, Polym. Degrad. Stab. 93 (2008) 1323–1331.
[35] B. Ramaraj, S.K. Nayak, K.R. Yoon, J. Appl. Polym. Sci. 116 (2010) 1671–1677.
[36] D. Chen, X. Wang, T. Liu, X. Wang, J. Li, Electrically conductive poly(vinyl alcohol) hybrid films containing graphene and layered double hydroxide fabricated via layer-by-layer self-assembly, ACS Appl. Mater. Interfaces 2 (2010) 2005–2011.
[37] S.E. Mallakpour, A.R. Hajipour, S. Habibi, J. Appl. Polym. Sci. 86 (2002) 2211–2216.
[38] J.T. Kloprogge, L. Hickey, R.L. Frost, J. Raman Spectrosc. 35 (2004) 967–974.
[39] S. Miyata, Clays Clay Miner. 28 (1980) 50–56.
[40] E. Kanezaki, Mater. Res. Bull. 33 (1998) 773–778.
[41] R. Vincente, Study of layered double hydroxides by thermal methods, in: Layered Double Hydroxides: Present and Future, Nova Science Publisher, New York, 2004, pp. 115–137 (Chapter 4).
[42] M. Jakupca, P.K. Dutta, Chem. Mater. 7 (1995) 989–994.
[43] L. Pesic, S. Salipurovic, V. Markovic, D. Vucelic, W. Kagunya, W. Jones, J. Mater. Chem. 2 (1992) 1069–1073.
[44] J.C.A.A. Roelofs, J.A. van Bokhoven, A. Jos van Dillen, J.W. Geus, K.P. de Jong, Chem. Eur. J. 8 (2002) 5571–5579.
[45] J.W. Gilman, Appl. Clay Sci. 15 (1999) 31–49.
[46] U. Wagenknecht, B. Kretzschmar, G. Reinhardt, Macromol. Symp. 194 (2003) 207–212.